Department for
Energy Security
& Net Zero

LEEDS BECKETT UNIVERSITY
LEEDS SUSTAINABILITY
INSTITUTE

DEEP Report 2.01

Case Study Methods

October 2024

Prepared for DESNZ by

Professor David Glew, Leeds Beckett University (LBU)

LBU contributing authors (alphabetically):

Mark Collett
Dr Martin Fletcher
Dr Adam Hardy
Beth Jones
Dominic Miles-Shenton
Dr Kate Morland
Dr Jim Parker
Dr Kambiz Rakhshanbabanari
Dr Felix Thomas
Dr Christopher Tsang

Any enquiries regarding this publication should be sent to us at: EnergyResearch@energysecurity.gov.uk

Contents

Executive summary

This report describes the common data collection and analysis methods used in the DEEP retrofit case studies. These are generically described to avoid repetition in the individual case study reports.

Three general methods are used to evaluate the DEEP case study buildings and the performance and risks of the different retrofits:

- in-situ field trial measurements in homes in the UK
- whole house energy modelling, and
- elemental thermal modelling.

The field trials provide a detailed data set that enables an exploration of the critical issues in undertaking retrofits. Specifically, when piecemeal (as opposed to whole house retrofits) take place. In broad terms the field trials seek to understand, at the deepest level possible, the complexities and interconnectedness involved. This understanding forms the bedrock of the evaluation of such things as benefits, unintended consequences, cost effectiveness, and improved modelling.

The modelling work complements the field work; energy models are updated to improve the quality of their inputs, forming a calibration of sorts:

- airtightness tests to update infiltration inputs,
- heat flux measurements to update U-value inputs, and
- elemental thermal modelling outputs to update thermal bridging heat loss inputs.

This approach explores the importance of using accurate model inputs (rather than default assumptions), by comparing predicted modelled retrofit performance and risk of retrofits to measured values.

Additionally, differences between the steady-state and dynamic energy models used are also compared, along with investigating the implications of RdSAP's restricted range of default inputs on model accuracy.

1. Introduction to DEEP case studies

In the DEEP project, thirteen individual methods were employed on each case study home, under three broad research approaches of: 1) in-situ measurements, 2) energy modelling, and 3) thermal modelling.

Case study research is preferred in this project since deep dives into a small number of field trials will provide the most useful data to answer the project's exploratory research questions. This approach has been previously used to extract rich data on retrofitting homes, that can be applied more broadly [1]. DEEP case studies still represent the largest single set of intensive retrofit Building Performance Evaluations (BPE) ever undertaken in the UK.

Case studies were limited to solid walled homes, since these are often the most challenging to retrofit to the EPC band C target, and their occupants are more likely to be in fuel poverty [2]. Within this sub sample, effort was made to select a range of building forms, construction types, and material properties for investigation, in order to maximise relevance for the UK housing stock.

1.1. DEEP case study objectives

Fourteen DEEP case studies, collectively, will attempt to investigate research objectives listed in Table 1-1, though not all the objectives are addressed by each case study.

Table 1-1 DEEP research objectives

Objective	Rationale
Model input accuracy	Policy relies on models with known limitations; exploring inputs and model robustness will improve policy advice.
Unintended consequence	More retrofit scenarios need modelling to confirm condensation, underperformance, air quality, and comfort risks.
Cumulative impact	Piecemeal retrofits are common; clarity is needed on the impact of different options, including achieving EPC band C.
Fabric vs ventilation	Insulation influences fabric and ventilation heat loss yet models currently only attribute savings to U-value changes.
Floor retrofit	80 % of homes have uninsulated floors; clarity on benefits may increase installation from 0.5 % of ECO measures.
Airtightness retrofit	Infiltration undermines retrofits; balancing airtightness and indoor air quality is an unexploited ECO opportunity.
Neighbour risk	Studies will investigate if whole house or staged retrofits affect condensation risk for neighbours.

1.2. Case study research questions

Over the course of the project and following advice from DESNZ, the wider DEEP Steering Group, and expert QA panel, additional questions were proposed. The objectives were refined to develop seven discreet research questions. These are listed below and used in discussing the findings:

1. *What combinations of retrofits are needed to bring solid walled homes up to an EPC band C? Do these represent value for money and what challenges do they face?*
2. *To what extent do unintended consequences reduce energy efficiency savings and increase moisture risks, when insulating solid walled homes?*
3. *Are methods to reduce the potential risk of unintended consequences, when retrofitting solid walled homes, effective and appropriate?*
4. *How significant is airtightness in domestic energy efficiency? Is improving airtightness a practical, low-risk retrofit measure for inclusion in domestic energy efficiency policy?*
5. *How accurate can energy modelling of retrofits be? How can EPCs be improved for use in retrofit performance prediction?*
6. *How can thermal modelling support risk management and retrofit energy modelling predictions?*
7. *How effective are low pressure Pulse tests and QUB tests as alternatives to the blower door test and the coheating test?*

1.3. Case study research design

To answer the research questions, a consistent strategy for data collection and analysis was adopted for each case study. Three research approaches were adopted:

- in-situ measurements;
- whole building energy modelling;
- elemental thermal modelling

These methods were combined to understand how retrofits affect whole house heat loss via fabric plane element, ventilation, and thermal bridging heat losses, as well as understand surface condensation risks.

The field trial investigations used a range of building performance evaluation (BPE) techniques to collect measured data; to provide an understanding of actual performance (at every stage in the retrofit process), against which modelled predictions can be compared.

Steady-state and dynamic whole building energy modelling tools were used to investigate whole house heat loss in DEEP:

Steady-state models

- Building Research Establishment Domestic Energy Model (BREDEM) 2012, on which the Standard Assessment Procedure (SAP) model is based, and which produces Energy Performance Certificates for new build homes [3]
- Reduced Data SAP (RdSAP) v9.9.4: a simplified software used to standardise the way BREDEM can be used to generate EPCs for existing homes

Dynamic energy model

- The DesignBuilder dynamic simulation modelling (DSM) software, which uses EnergyPlus as its physics engine [4]

These have all been subject to academic and industry scrutiny, and the fundamental physics of their calculation methods is robust [5-9].

To investigate thermal bridging heat losses and condensation risk analysis, thermal modelling and simulation was undertaken on the case study dwellings using Physibel's TRISCO software, version 15.0.01 [10].

Currently, PAS 2035 guidance for retrofits discusses the use of models in retrofit design and evaluation. It specifies that Retrofit Assessors, Designers and Coordinators should be familiar with whole energy building models [11], modelling of risk-critical features such as thermal bridges, and the use of TM59 [12] to assess overheating risk. This indicates that RdSAP, BREDEM (i.e. the engine behind full SAP), and DSM, as well as thermal modelling, should inform retrofit design.

Thus, the modelling work, in conjunction with the in-situ measurements, provides a holistic deep dive investigation into each case study home. An overview of these methods is given in the next section.

1.4. Case study methods overview

The common methods used across all the case studies are described in this report to avoid repetition in the individual field trial reports, and they are summarised in Table 1-2. Any variations from or adaptations to these methods are discussed in the field trial reports. Each specific method is discussed in detail in the following sections.

Table 1-2 Overview of DEEP case study methods

Research	Method	Output	Reference
1. In-situ measurement	1.1 Coheating test	Heat Transfer Coefficient (HTC)	[13]
	1.2 QUB & QUB/e	HTC, U-values	[14-16]
	1.3 SmartHTC (SMETER)	HTC	[17]
	1.4 Blower door tests	Air leakage rates Background ventilation heat loss (HTC_v)[1]	[18]
	1.5 Pulse test	Air leakage rates	[19]
	1.6 CO_2 decay	Air leakage rates	[20]
	1.7 Heat flux measurements	U-values Fabric heat loss (HTC_f)	[21]
	1.8 Thermocouple measurements	Temperature factor surface condensation analysis	[22]
	1.9 Thermography	Qualitative assessment of surface temperatures Air leakage paths	[23]
2. Energy models	2.1 RdSAP	HTC Annual heating demand Annual fuel bills Annual carbon emissions	[24]
	2.2 BREDEM		[25]
	2.3 DesignBuilder (DSM)		[4]
3. Thermal models	3.1 TRISCO	Thermal bridging heat loss (HTC_b) Temperature factor surface condensation analysis	[10, 26, 27]

[1] Assuming the n/20 Kronvall-Persily rule of thumb

2. In-situ measurements

The DEEP project undertook deep dive case studies to investigate domestic retrofits, using a range of established building performance evaluation (BPE) in-situ *tests in collaboration. These are described in detail here.*

2.1. Coheating test

The coheating test remains the most reliable method to measure aggregate whole building heat loss, and is widely used in buildings research [17]. The coheating test has been designed to calculate the steady-state heat loss through the thermal envelope of a building. To achieve this, a stable and elevated internal temperature is reached within a property. As the property will then lose heat to the external environment, additional power will be required to maintain the internal temperature. This power is recorded, along with the internal and external temperatures. For each 24-hour period of the coheating test, the average power use is calculated, along with the difference in the average internal and external temperature (ΔT).

Plotting this power use against ΔT should yield an approximately straight line. A linear fit to these points will reveal the gradient of this line, which can be taken as the estimate of the Heat Transfer Coefficient (HTC), with units of W/K.

Full details of the coheating test protocol can be found in reference [13]. The DEEP project makes one notable update to the analysis procedure described in the coheating test protocol: by replacing a standard *linear regression* algorithm for one using *Deming regression [28]*. Linear regression algorithms typically assume there is no uncertainty in the ‘x’ axis variable (in this case, daily mean ΔT). For a coheating test there will, of course, be some uncertainty associated with the ΔT value. To account for this, the coheating analysis used in the DEEP project first quantified this uncertainty. The analysis then used a regression algorithm (Deming regression) which can consider an uncertainty in the x axis variable (ΔT).

To estimate the uncertainty in the ΔT variable, some consideration needs to be given to how ΔT is calculated. In its simplest form, the time average for the mean external air temperature is calculated over a 24-hour period. This value is subtracted from the time average of the internal air temperature over each 24-hour period. However, the internal temperature is monitored in multiple locations, and all of these must be considered in the average internal temperature.

Before averaging over time, the internal temperatures are therefore averaged over space. A small space may overheat during coheating, without affecting the final HTC significantly. To account for this, a weighted average is used when averaging over space, with the weights set at the room volumes. This has the effect that large rooms contribute more to the average house temperature than small rooms. If data from multiple external temperature sensors are available, these are combined with a simple mean average and no weighting is applied.

The time series for internal and external temperatures do not follow any typical probability distribution, and this precludes the use of any simple equations to calculate the uncertainty. Instead, a bootstrap procedure was employed. This involves resampling the time series data thousands of times and recalculating the mean for each of these samples. The distribution of these ‘simulated’ means can then be used to characterise the uncertainty in the mean temperatures.

Unsurprisingly, the uncertainty in the average internal temperature was found to be very low in our experiments, suggesting that the internal temperature was controlled successfully. This is not the case for the external temperature: days with large external temperature variations can result in a large uncertainty on the mean ΔT found through a bootstrap procedure. Note that we do not consider sensor measurement uncertainty, though sensors were checked for drift that may have occurred over time. Sensor measurement uncertainty was calculated to be insignificant, owing to the very large number of data points collected (the coheating test takes at least two weeks, for full details about the coheating test, please refer to [13]).

2.2. QUB

QUB, unlike the quasi-static coheating test, is an in-situ dynamic measurement method to determine the as-built HTC of dwellings within a single night without occupancy. QUB was developed by Saint-Gobain and has been tested and validated in the UK and Europe. Currently there is no formal standard for the procedure, hence the procedure undertaken was based on guidance from Saint-Gobain and as detailed in validation studies [14-16].

The test procedure takes place overnight and consists of two distinct phases of equal length: a constant heat injection phase, followed by a free cooling phase. Throughout the test, internal and external temperatures and power inputs are monitored to determine the thermal response to both phases. The recorded data can be used to identify the parameters in Equation 1 and compute the HTC.

Equation 1

$$HTC = \frac{T_2' P_1 - T_1' P_2}{T_2' \Delta T_1 - T_1' \Delta T_2}$$

where subscripts 1 / 2 indicate the measurements taken at the end of the heating / cooling phase respectively, T' is the slope of the temperature profile, P is power input and ΔT is the internal / external temperature difference. Where multiple QUB tests were undertaken on consecutive nights, a pre-heating step was included to ensure optimal starting temperature resulting in an α value of between 0.4 and 0.7 [14]. α is a dimensionless parameter that characterises the required heat input, P_1 against the internal / external temperature difference at the start of the test ΔT_0, and the predicated HTC of the building H_{ref}. This is calculated through Equation 2.

Equation 2

$$\alpha = 1 - \frac{H_{ref} \Delta T_0}{P_1}$$

The uncertainty of the HTC measured through QUB is calculated through Taylor Series Method (TSM) for Uncertainty Propagation.

2.3. Blower door test

Airtightness tests were undertaken on all test houses by the Leeds Beckett research team using the fan pressurisation method described in ATTMA Technical Standard 1 (2016). Although this standard was superseded by CIBSE TM23:2022 *Testing buildings for air leakage* (2022) during this project, the methodology remained as only calibration requirements differ between the two protocols. Deliberate ventilation openings (e.g. background ventilators) were sealed, all interior doors opened, and an Energy Conservatory Minneapolis Model 3 Blower Door™ System with a DG-700 pressure/flow gauge was used. Tests were conducted at a range of internal to external pressures, with the results reported being a mean of pressurisation and depressurisation tests at 50 Pa.

Tests were repeated for every dwelling at critical stages of each retrofit process, to assess changes in the airtightness performance as the retrofits progressed; allowing informed calculations of background ventilation heat loss at each stage to be compared. Tests were performed immediately after coheating tests, to ensure that any disaggregation of heat loss was using the value closest to that experienced during the test.

Tests were generally performed with the blower door positioned in the most sheltered doorway, avoiding the prospect of strong wind directly onto the blower door, and thus increasing the likelihood that the same doorway could be used throughout the retrofit process. The depressurisation phase of each test was carried out first, to allow infiltration detection to be conducted immediately following this, using an infra-red thermal imaging camera, followed by the pressurisation phase. Leakage detection relied on a $\Delta T \geq 10$ K and was conducted with the house depressurised by ~50 Pa relative to external.

Additional ‘Spot50Pa’ measurements were regularly recorded as part of a blower door test to estimate the change caused by a single action or variation, such as sealing a leaky window or opening a closed vent. The Spot50Pa measurements involved taking the mean of several 10 second average measurements at ~50Pa under just depressurisation or pressurisation, rather than performing an additional full blower door test.

Variations to this procedure were necessary on a few occasions. Where higher pressures risked damaging temporary or partly constructed work/sealing, blower door tests were conducted between 15 and 50 Pa rather than the usual 20 to 70 Pa. Similarly, occasionally, when it was considered that either the pressurisation or depressurisation phase of the test might risk causing damage to the house, the test was performed using just the other phase.

2.3.1. Thermographic leakage detection

Thermographic inspections for air leakage detection in houses were undertaken throughout the project whenever site visits were carried out and both internal and external environmental conditions deemed suitable. Thermographic images were captured using either a Flir B620, Flir T660, or Flir T1K infrared thermal imaging camera. Thermographic leakage detection under dwelling depressurisation was performed immediately following the depressurisation stage of each airtightness test whenever there was a sufficient internal/external temperature differential ($\Delta T \geq 10K$).

2.3.2. Co-pressurisation tests using blower doors

During blower door tests some air movement in the recorded aggregate infiltration rate is actually movement between dwellings. Air exchange between neighbouring homes might not represent a heat loss since both homes may be heated. Therefore, when using blower door tests to understand heat lost to the outside, it is useful to remove the inter-dwelling air exchange by undertaking a co-pressurisation test (i.e., holding all adjoined dwellings at the same pressure while undertaking the pressurisation test and removing drivers for inter-dwelling exchange).

Co-pressurisation tests were carried out on several attached houses. While airtightness tests on individual dwellings induce pressure differences on all elements of the building envelope, co-pressurising removes the pressure difference across a party/separating element. The infiltrating air from an attached house is not external air but has already been conditioned by the neighbour.

Co-pressurisation tests involve performing airtightness tests on two neighbouring houses simultaneously. Readings are only recorded when the internal/external pressure differentials in both houses are similar (<1.0 Pa difference). An example set-up is shown in Figure 2-1. In unoccupied houses it was possible to conduct full pressurisation tests according to the ATTMA Technical Standard 1 (2016) protocol in both houses simultaneously. Where the neighbouring house was occupied, it was sometimes judicious to undertake just depressurisation (or even Spot50Pa) measurements to avoid occupant discomfort and disturbance.

Figure 2-1 Blower doors in adjoining dwellings during co-pressurisation test

2.4. Low pressure Pulse test

Low pressure Pulse tests were undertaken at various stages of each retrofit process and were conducted using the BTS Model 1 Pulse Test system. This was provided by Build Test Solutions Ltd, and tests conducted using the method described by Cooper, Zheng, et al. (2019). This method has since been adopted as an accepted test methodology for new build dwellings in CIBSE TM23:2022 (2022) as the ‘low pressure Pulse - LPP method’ but has yet to gain acknowledgement as an accepted method for testing existing dwellings.

The Pulse test measures air leakage/exfiltration at lower pressure differentials than the blower door test, meaning conditions are more like those naturally experienced. However, the Pulse test only measures under pressurisation (not depressurisation) and does not allow any leakage detection to be undertaken to identify air leakage paths.

The Pulse method was originally developed to investigate building envelopes of single zone buildings, hence the methodology used demanded all tests were undertaken with all internal doors opened to allow pressures to equalise throughout these multi-zone dwellings. This method has provided consistent results for new-build UK homes (Zheng, Cooper, et al., 2019). However, with the more variable airtightness characteristics of some existing dwellings it has proved to be less reliable, i.e. smaller, simpler, more airtight homes may deliver more reliable results than larger, more complex, and leakier homes.

Known complexities that can cause uncertainty include buffer zones between the internal and external environment; for example, attic knee walls, cellars, and suspended timber floor voids regularly caused acoustic interference [17]. The BTS Model 1 Pulse Test system used in this project comprised of a 40-litre air receiver with a 60-litre expansion tank for use when required. However, with the size of some of the properties, and their low levels of airtightness, this was sometimes insufficient to achieve the necessary pressures required for the Pulse analysis (https://www.Pulseairtest.com/sizing-guide.html).

2.5. CO_2 Decay

BS EN ISO 12569:2017 outlines three methods of using tracer gases to determine the air leakage of a building. Two of the methods: continuous dose method and constant concentration method, necessitate highly accurate measurement of the gas injected. For this reason, the third was utilised: concentration decay method, which examines the rate at which an injected gas concentration falls; requiring only measurement of the tracer gas concentrations.

Air change rates were calculated using CO_2 as a tracer gas using the method described by Roulet and Foradini (2002), allowing a ventilation measurement to be conducted using no artificially induced internal pressures to measure the natural rate of concentration decay.

A timed release of CO_2 was administered on the ground floor of the test house during the night, to raise the CO_2 concentration of the internal air significantly above atmospheric levels. Eltek GD47 CO_2/Temp/RH sensor/transmitters were positioned on the ground and top floors, recording the internal CO_2 concentrations at 1-minute intervals. Air change rates were calculated by analysing the concentration decay over a 30-minute period, selected after a maximum 1-minute decay at that sensor had been measured. The background concentration used was based on the CO_2 concentration recorded over the thirty minutes immediately prior to the timed release.

The period from maximum CO_2 concentration being recorded on the ground floor to maximum concentration on the top floor, and the difference between the peak concentrations at each, gave insight into ventilation mechanisms experienced during the test phases. This was not, however, used in any quantitative analysis. Data collected during periods of unstable background concentration or highly changeable external atmospheric conditions were also excluded from any analysis.

As with the Pulse tests, the values obtained by the CO_2 decay investigations were used only to generate useful comparison data to the blower door test, not to inform any of the heat loss investigations elsewhere in DEEP.

2.6. Heat flux density measurements

Heat flux through different elements of the building was measured using Hukseflux heat flux plates (HFPs) and a DataTaker logger (either a model DT80 or DT85M). The purpose of these heat flux measurements was two-fold.

In the first instance, these readings allowed the U-value of the element to be estimated when combined with data on the internal and external temperature. The BS ISO 9869-1 average method was used to calculate these U-values. Where this was not possible (due to the system being too dynamic and/or the surface being exposed to solar radiation), a dynamic method was employed instead. This modelled the system as a resistor–capacitor (RC) circuit and used stochastic modelling to derive the physical parameters of the circuit [29]. The RC method was shown to agree with the ISO method. This dynamic method follows similar principles to those detailed in ISO 9869-1:2014 Annex B. However, where the ISO 9869 creates a large system of linear equations that require solving, the dynamic method models the system as an electrical circuit and solves the parameters using a continuous time stochastic model. This approach allows for the inclusion of solar radiation into the model and is therefore particularly suitable on elements that are likely to experience sun-induced temperature fluctuations. On elements with little solar, our dynamic model shows excellent agreement with results from the ISO 9869 model. Given the short testing programme it was not possible to undertake any mitigation activities to reduce the amount of solar radiation or rainfall.

In the second instance, the HFP measurements were used to adjust the coheating data to account for party wall (PW) heat loss. The HTC of a property is defined using heat loss to the external environment. However, unless the property is detached, some of the power will be lost to neighbouring dwellings. This power therefore needs to be subtracted from the power input to the property if an accurate HTC is to be calculated. To perform this, a thermal camera was used to inspect the PW in each room of the property. If the surface appeared homogeneous in the IR image, a HFP was fixed to the wall in a location deemed to be representative of the surface (typically in the centre of the wall). If the surface appeared inhomogeneous, multiple HFPs were placed to account for this. For each HFP, the area which it represented in m^2 was calculated. The HFPs collect data in units of W/m². Therefore, multiplying the data collected by the HFPs in their representative areas resulted in a power loss through that PW element. The sum of these PW element losses was subtracted from the coheating data to account for the PW heat loss.

For both applications, an error was discovered in the data collection process. The DataTaker DT85s were found to be experiencing ‘ground loops’ in some instances (note that DT80s are shielded from this phenomenon). Ground loops appear when two or more points on a circuit are connected to the ground.

This creates a conductive loop through which current can flow. The oscillating current of UK power supplies can then induce a small potential within this loop, adding a small voltage to that which the sensor is truly measuring. The extent of these ‘offset’ voltages is dependent on the specific experimental setup, and therefore changes with every house. However, an investigation into the phenomenon determined that for a specific house, the offset value is stable over time. For each home in which a DT85 was used, an offset voltage was therefore calculated by comparison to data from a DT80 HFP on the same element. A 95 % confidence interval was also calculated for this offset and propagated through the analysis of both U-values and coheating HTCs. If an offset could not be calculated, the data from that DT85 was not used.

2.7. Thermocouple measurements

Surface temperature measurements were undertaken at locations in the building fabric where thermal bridging was expected to occur. This included junctions in the external building envelope as well as areas where discontinuities were expected to occur within the retrofit. These surface temperature measurements, alongside internal and external air temperature, were used to calculate temperature factors (f_{Rsi}) using Equation 3.

Equation 3

$$f_{Rsi} = \frac{T_{Si} - T_e}{T_i - T_e}$$

where T_{Si} is the internal surface temperature, T_e is the external air temperature and T_i is the internal air temperature. For domestic properties, a modelled temperature factor below 0.75 in steady-state conditions is taken to indicate that there is an unacceptable risk of condensation forming under normal occupation [22].

Surface temperatures were measured with T-type thermocouple sensors, which were fixed to locations of interest in the test dwellings. Fixing was made by applying a small amount of heat sink compound to the end of the sensor, then attaching it to the wall with reflective foil tape to reduce the effects of radiant heat from coheating equipment on the surface temperature readings. Each thermocouple was connected to an Eltek GS-24, which transmitted temperature readings to the central data logger.

The quasi-steady-state conditions of a coheating test provide an environment that is comparable to the steady-state numerical thermal models used to evaluate thermal bridging and moisture risk at junctions of the building fabric. While the internal temperature can be controlled, the external temperature and its fluctuations due to weather cannot. To ensure that the values of f_{Rsi} obtained from surface temperature data were not unduly influenced by transient heating and cooling due to the external environment, the Averaging method within BS ISO 9869-1 [21] was adopted to validate the stability of each value of f_{Rsi}.

Average temperature factors were calculated for each 24-hour period, beginning at 06:00 to 05:59 the following day. This approach limits the heating and cooling due to solar exposure each day to a single 24-hour period. An average of the 24-hour f_{Rsi} values can then be calculated using the following selection criteria:

- **1st Test:** The time period for the test must be greater than 72 hours
- **2nd Test:** The f_{Rsi} value of the last 24-hour interval must be within ±5% of that obtained from the previous 24-hour interval
- **3rd Test:** The value of f_{Rsi} calculated over the first X 24-hour intervals is ±5% that calculated over the final X 24-hour intervals

where X is: (2 x Total number of 24-hour intervals / 3)

Where the three tests cannot be satisfied, the monitored data is considered too unstable.

In-situ measurements summary

A range of in-situ measurements were used, which provided a deep dive investigation into the benefits of retrofits in the case study homes and ensured that the differences in performance and risk could be measured when considering piecemeal versus whole house approach retrofits.

Data collected on surface temperatures pre-retrofit and post-retrofit was utilised to explore how condensation risk in the case study homes was affected by retrofits.

Alternative approaches to measuring in-situ data have also been adopted to provide insights into the robustness of novel measurement techniques.

The proposed techniques are designed to give an understanding of the different heat losses attributed to fabric and ventilation heat losses.

3. Elemental thermal modelling

Thermal modelling of DEEP case study buildings was undertaken for two purposes: 1) to evaluate the condensation risk that different retrofit scenarios present by calculating the temperature factor (f_{Rsi}) for junctions, which could also be compared to risk as assessed through in-situ surface temperature measurements; and 2) to calculate linear transmittance or Ψ value (Psi value) of junctions in case study homes, to understand the whole house thermal bridging heat losses (HTC_b), and to support the calibration of the energy models. The appropriateness of default data of construction material properties used in thermal bridging modelling was assessed by substituting the tabulated material properties with measured construction material properties, which were derived from laboratory analysis of core samples taken in the case study homes.

3.1. Introduction to elemental thermal modelling

Thermal bridging affects surface condensation risks and heat loss, yet it remains one of the largest unknowns in energy modelling and retrofit risk assessment. The approach taken in DEEP to investigate the extent to which both are affected by retrofitting homes is discussed in this section. Several key technical terms and equations are used:

U-value: the rate of heat transfer through a plane element of a building fabric (i.e. homogenous or repeating elements such as walls, floors, or roofs) per square metre, per kelvin temperature difference between internal and external air temperature. The unit for U-value is W/(m²·K).

Ψ (Psi) value: the measure of linear thermal transmittance: heat lost at the junction between two plane elements of a building's thermal envelope. The unit is W/(m·K) and is the rate of thermal energy in watts lost per metre length of junction per kelvin difference between internal and external air temperatures.

λ (lambda): the thermal conductivity of a material. The unit is W/(m·K) and is the rate of thermal energy in watts transferred through a thickness in metres of material per the difference in kelvin on either side of the material.

R-value: the thermal resistance of a given layer of material, of a given thickness, derived by dividing the thickness of a material layer (m) by the thermal conductivity of the material. The higher a material R-value the greater its insulating effect. The unit is m²·K/W.

f_{Rsi}: temperature factor: a ratio used to indicate whether there is a risk of surface condensation and mould growth at a junction. In domestic buildings a value below 0.75 is taken to indicate that the junction is at risk of condensation or mould growth with lower values considered to indicate a greater risk. f_{Rsi} is calculated using Equation 4:

Equation 4

$$f_{Rsi} = \frac{T_{si} - T_e}{T_i - T_e}$$

where T_{si} is the lowest internal surface temperature, T_e is the external air temperature, and T_i is the internal air temperature.

$\boldsymbol{HTC_b}$**:** The heat transfer coefficient for a whole building associated with thermal bridges is the sum of the length of each linear thermal bridge, multiplied by the Ψ-value at that thermal bridge. Where Ψ-values are known HTC_b is calculated using Equation 5:

Equation 5

$$HTC_b = \sum (L \times \Psi)$$

where L is the length of the thermal bridge, in metres, over which Ψ applies.

Where the Ψ-values of thermal bridges within a dwelling are unknown, an estimated HTC_b can be calculated using a y-value, as in Equation 6:

Equation 6

$$HTC_b = y \times A_{ext}$$

where A_{ext} is the total area of external elements, and y = 0.15 W/(m²·K)

y-value: If details of the thermal bridges within a building are not known, a simplified method is often used. A default y-value of 0.15 W/(m²·K) is used in RdSAP. A y-value can also be derived by dividing a known HTC_b by the total area of external elements, as shown in Equation 7.

Equation 7

$$y = \frac{HTC_b}{A_{ext}}$$

where HTC_b is determined as in Equation 5 and A_{ext} is the total area of external elements.

To include HTC_b in BREDEM models 3 different y-values were used:

- default y-value
- y-value based on SAP appendix K Ψ-values
- y-value based on Ψ-values derived from elemental thermal modelling

3.2. Elemental thermal modelling method

Elemental thermal modelling of the linear thermal bridges was undertaken following guidance from BR 497 [26]. Where deviations from this guidance were made, it is noted in the relevant report. Each linear thermal bridge was modelled in the pre-retrofit state and at each stage of retrofit that the building being assessed underwent. In addition, some further models were created representing alternative retrofit sequences that did not occur during the case study.

The process of creating models and calculating Ψ-values is described in this section.

3.2.1. U-value calculation

To calculate the Ψ-value of a linear thermal bridge, the U-value of the flanking plane elements must be calculated. U-values were calculated following guidance in BR443 [30]. U-values of plane elements other than ground floors were calculated using TRISCO ver. 15.0.01 [10]. For plane elements composed of homogenous layers (e.g. a brick wall) a 1 m² model was created. Where a plane element consists of inhomogeneous repeating layers (e.g. a ceiling with timber rafters), a model representing the smallest symmetrically repeating unit of that element was created. The resulting model will often have an area less than 1 m².

Thermal models were divided into nodes using the TRISCO software's auto split function and a simulation run. The resulting value of Q (total heat flow out of internal boundaries) was used to calculate a U-value for the plane element using Equation 8:

Equation 8

$$U = \frac{Q/a}{T_i - T_e}$$

where: Q – Is the rate of heat flow out of internal boundaries, in watts (W)

a – is the area of internal surfaces (m²)

T_i – is the air temperature of the internal boundary condition (°C)

T_e – is the air temperature of the external boundary condition (°C)

The U-values of ground floors were calculated using the BRE U-value calculator [31]. The floor build up was set up to match the floor as-built; dimensions of the floor were set to a notional square floor with a characteristic length of 8m per side and the exposed perimeter-to-area ratio to 0.25, following the guidance of BR 497.

3.2.2. Linear thermal bridging calculation

Ψ-values of linear thermal bridges were calculated following the guidance of BR 497 using numerical thermal simulation software (TRISCO). For each junction, a model was created within the software, consisting of the linear thermal bridge and the adjoining flanking elements. The geometry, materials, and construction of each model used on-site observations and measurements. Where it was not possible to gain access to parts of a junction, assumptions were made based on observations elsewhere in the building and typical constructions.

Where a build-up of a thermal bridge was homogenous along its length, the model was created to be 1 m in the axis of the thermal bridge. Where repeating elements were present, the model was created to represent the least repeating unit of the thermal bridge, and the length was set to match the least repeating unit.

Boundary conditions for each model were set to 0 °C externally and 20 °C internally. Surface resistances were set depending on the horizontal or vertical orientation of the surface and direction of heat flow, according to guidance in BR497. Where a large, sheltered, unheated void was present (such as in the eaves at 17BG), the boundary condition in the void was set to 0 °C, but the surface resistance was set as if the space was internal. For suspended ground floors, the under floor void temperature was determined according to Annex G of EN ISO 13370, using the BRE U-value calculator. This value was used as the under-floor boundary condition.

Once complete, each model was divided into nodes using the auto split function in TRISCO. This process refines the number of heat transfer nodes to give an optimum level of detailed simulation, without overloading the computational capability of the software and hardware. Once divided, each model was run, simulating the heat flow through the modelled thermal bridge under steady-state conditions. Three main outputs were taken from this simulation:

- A visual representation of the temperature distribution throughout the model
- Q, the heat flow in watts out of the internal boundary conditions
- T_{min}, the minimum internal surface temperature

To determine the Ψ-value of a linear thermal bridge, firstly L^{2D} (the thermal coupling coefficient, the heat loss in watts per degree difference between internal and external temperature) is determined, using Equation 9.

Equation 9

$$L^{2D} = \frac{Q}{T_i - T_e}$$

The resulting value of L^{2D} is then used to calculate the Ψ-value of the thermal bridge, subtracting the heat flow through the flanking plane elements from L^{2D} using Equation 10.

Equation 10

$$\Psi = \frac{L^{2D} - \sum(U \times a)}{l}$$

Where: U is the U-value of each flanking plane element

a is the surface area of each flanking plane element (m²)

l is the length of the modelled linear thermal bridge (m)

Equation 10 expresses the general method of determining the Ψ-value at a thermal bridge. Some more complex junctions require a variation of Equation 10. Where this was the case, the guidance of BR 497 was followed.

3.2.3. External Ψ-values

In addition to calculating Ψ-values following the guidance of BR 497 (which uses internal dimensions to determine lengths and areas), external Ψ-values were calculated, which use external dimensions to calculate lengths and areas. Other than the dimensions used, the calculation methods for external Ψ-values are the same.

External Ψ-values tend to be lower than internal Ψ-values in most contexts. However, they are used in conjunction with external measurements for heat loss areas. Overall, internal and external methods of calculating fabric heat loss should result in the same value. External Ψ-values are used in some assessment packages, including Dynamic Simulation Modelling software and PHPP (Passivehaus Planning Package) which are programmed to use external Ψ-values.

3.2.4. Material thermal properties

Each material used in the numerical thermal simulation models was assigned a thermal conductivity (λ). Values of λ were assigned in an order of preference; where possible, manufacturer-declared values of λ were used. Where these were not available, a value was taken from BR 443 [30]. Lastly, values from BS EN 10456 [32] were used.

Equivalent λ values were determined for the air cavities in models, based on the dimensions and direction of heat flow through the air cavity. The Kornicki Air Cavity Calculator [33] was used to perform these calculations.

λ values for brick walls were calculated based on the observed brick bond pattern of each house and standard λ values for bricks and mortar. Proportions of brick and mortar in the inner and outer leaves of the solid wall were determined based on the minimum repeating brick bond pattern. An equivalent λ was then calculated. An equivalent λ for the centre joint between the inner and outer leaves of brickwork was also calculated. The proportion of header bricks within the cavity was determined based on the brick bond pattern. The remainder of the centre joint was assumed to be made up of mortar and air cavities, the proportion of which was based on the findings of Hulme et al. [34].

Measured thermal conductivities of bricks were also used to refine the equivalent λ values for the solid brick walls, replacing the standard λ values for bricks with those measured for each house. The method of measuring the λ value of bricks for each house is detailed in DEEP Report 4, Brick material properties.

Variants of each thermal bridge model featuring the external brick wall were created using equivalent λ values for the brick walls calculated using measured brick λ. This was done to assess the impact of measured thermal properties for the existing construction on the resulting Ψ-values, HTC_b and condensation risk at thermal bridges.

3.3. Modelled surface condensation risk

The surface condensation risk at each junction and at each stage of the case study was assessed by calculating the temperature factor (f_{Rsi}). This was based on the minimum internal surface temperature simulated by each numerical thermal simulation of the linear thermal bridges in the case study houses (see previous sections for the methods used).

Using Equation 4, the minimum internal surface temperature for each scenario, along with internal and external boundary condition temperatures, were used to calculate f_{Rsi} at each thermal bridge. Where a f_{Rsi} below the critical temperature factor (f_{CRsi}) of 0.75 [22] is calculated, this indicates that the thermal bridge is at risk of surface condensation formation. A 0.75 f_{CRsi} is used for domestic buildings, according to IP 1/06 [22].

Comparing the resulting values of f_{Rsi} for each retrofit stage (and additional scenarios) allows the condensation risk impact of piecemeal and deep retrofit approaches at each thermal bridge to be compared. This allows exploration of the relative risk of single interventions and a whole house approach.

3.4. Whole house thermal bridging heat loss

The contribution of heat loss due to thermal bridging at the whole house scale is represented as HTC_b, the heat transfer coefficient of all linear thermal bridges in the heat loss area of the building.

For each case study house where thermal bridges were assessed, three approaches were taken to calculate HTC_b: SAP 2012 appendix K [35] Ψ-values, modelled Ψ-values, and modelled Ψ-values using measured brick λ values. Firstly, all linear thermal bridges in the heat loss area of the house were identified and the lengths for each measured. Ψ-values were assigned to each thermal bridge; the Ψ-values varying depending on the approach being taken.

To calculate a HTC_b for a house using SAP 2012 appendix K, Ψ-values were assigned to each thermal bridge from matching junctions within appendix K. Where a specific match was not available within appendix K, the closest match was used instead.

When calculating a HTC_b using modelled Ψ-values, each thermal bridge was modelled as described in section 3.2.2. Ψ-values were calculated for each junction in each retrofit state.

To calculate a HTC_b for modelled Ψ-values using measured brick λ values, thermal bridge models were modified to include wall equivalent λ values based on measured brick thermal conductivities, as described in section 3.2.4. Ψ-values were then calculated for each thermal bridge.

Once Ψ-values had been assigned to each linear thermal bridge, a value for HTC_b was calculated by multiplying each thermal bridge Ψ-value by the length over which it applied and summing all heat losses, as described in Equation 5. This was carried out for each of the three approaches. The resulting values of HTC_b could then be used in DSM and BREDEM to assess the impact that the differing approaches to accounting for HTC_b would have on the predicted heat loss in these models.

Thermal bridging summary

This section described the methods used to assess linear thermal bridging in the case study houses that underwent whole house retrofits in DEEP.

Numerical thermal simulation software was used to model the thermal bridging at each junction in each retrofit stage that occurred during the test programme.

Ψ-values and f_{Rsi} were calculated for each thermal bridge. The resulting values were used to assess the changes in thermal bridging energy loss and condensation risk at each retrofit stage.

Ψ-values for each thermal bridge were used to calculate whole house heat loss due to thermal bridging (HTC_b) to assess the impact that different approaches to calculating HTC_b would have on the results of whole house energy models.

4. Energy modelling

Steady-state and dynamic whole building energy modelling software were used in DEEP. The performance of these were compared and the impact of using default versus specific model inputs were explored in DEEP.

4.1. Introduction to energy modelling

Models can generally be divided into two broad categories: data-driven models and physics-based models [36]. Data-driven models, as the name suggests, use data collected from a subject to develop predictions of how the subject will respond in the future. Conversely, the whole-building energy models used in DEEP are physics-driven models, where the underlying laws of physics are used to simulate thermal performance based upon model inputs. This is as opposed to data-driven models, which rely on historical data. It is also possible to combine these approaches, using real world data to calibrate physics-based models [36-39].

4.2. Whole building energy modelling software

Two types of energy modelling were used in DEEP: 1) Steady-state and 2) DSM. Steady-state models are the most widely used and generally the best understood. They are simple and used in policy and regulations. On the other hand, DSM models are more commonly used in research, since they have advantages in being able to simulate at small time-steps, and so consider how the building responds over the course of a few hours (or a day); therefore, they tend to be more accurate. It is important to note that this type of modelling can be sensitive to poor assumptions and human error [40]. It is, however, possible to address this using systematic approaches, and it has been shown as an effective means of estimating retrofit performance in the past [41-44]. There is, therefore, a trade-off between complexity and resource required versus model accuracy. There may indeed be an optimum level of complexity beyond which predictive accuracy does not improve. Currently it is estimated that by 2035 there could be a shortfall of around 25 % in the energy savings actually achieved through retrofit programmes compared to steady-state modelled predictions [45]. DEEP investigated if there are opportunities to improve the accuracy of both types of models.

4.2.1. Steady-state models; SAP, RdSAP & BREDEM

SAP is in essence a benchmarking tool that is used to estimate the energy demand of a house, based on the BREDEM calculation engine. It is often used to demonstrate compliance with Part L of the Building Regulations [46]. RdSAP is also based on BREDEM; however, the construction make-up of existing homes may not be known. To simplify and standardise the process for EPC assessors, RdSAP is used to place limitations on the inputs that can be varied and provides estimated age-band and construction-based default inputs for fabric, ventilation, and thermal bridging heat losses [24]. RdSAP is therefore the tool used when modelling existing buildings, i.e., when construction details are not available, while SAP is used for new build projects. Both are used to generate SAP ratings, EPCs, annual energy demand, fuel bill estimates, carbon emissions predictions, the whole house HTC, and the heat loss parameter (HLP). SAP is used to demonstrate compliance with Part L1A of the Building Regulations [46, 47].

Retrofits delivered via government schemes have historically required modelling to estimate savings, and most commonly specify the use of RdSAP [3, 6] to generate EPCs.

RdSAP has most recently been used in ECO but schemes such as the Feed-in Tariffs, the Renewable Heat Incentive and the Green Deal have also required RdSAP calculation outputs to evaluate financial viability [6].

Commercial software is available to undertake SAP and RdSAP models, though these have restrictions in the ability to alter inputs. Conversely, in BREDEM all the inputs and outputs can be directly altered. This is why it was selected for DEEP, as it gives greater potential to explore SAP in general. The RdSAP software package RSAP+, produced by STROMA, was used to understand the potential to improve models using existing software.

4.2.2. Dynamic Simulation Modelling (DSM)

The DSM models in DEEP were produced using DesignBuilder software version 7.0.0.088 [4] which uses Energy+ as its physics engine and allows for specific Psi (Ψ) value inputs to be used. DSM predictions of heat loss, energy use and retrofit savings for each case study home were compared against the steady-state models and measured data. It is also possible to derive the SAP score and, therefore, the EPC rating, annual energy demand, fuel bill estimates, carbon emissions predictions, the HTC, and the HLP. This means that DSM models can be directly compared to RdSAP and BREDEM outputs as well as the measured data. The DSM models can be set up to mimic the coheating test conditions, with model output data then used to calculate the HTC in the same way that in-situ measured data is used. This provides an alternative method of modelling the HTC to the steady-state calculation used in SAP.

4.2.3. Model input assumptions

To allow for meaningful comparison, all internal gains inputs for the annual energy modelling in DSM were calculated using the methodologies described in SAP specifically for each individual home. Most inputs relate to the total conditioned floor area of the dwelling, and in turn, number of assumed occupants and internal heat gain [48]. The total annual gains from occupancy, equipment, and lighting included in the different models were adjusted to closely match those used in SAP for each dwelling, in order to allow for a fair comparison to be drawn from the different modelling tools. Air changes related to purpose-provided ventilation were also taken from the SAP estimates and included in the total air changes per hour input, along with the background infiltration rate. A monthly schedule controls the air changes per hour in the DSM models, which takes account of the monthly wind speed factor included in the SAP calculations.

The fundamental difference between the dynamic and steady-state models is that DSM calculates at an hourly time-step. This is relevant to the operating schedules and building simulation weather data. In the SAP calculation, it is assumed that heating is operated for 9 hours per day on weekdays and for 16 hours per day at the weekend, as defined in Table 9 of the SAP methodology [48]. The heating operating schedules in DSM were set up to follow this standard pattern. Heating set-points in living areas were 21 ˚C and set points for other areas were calculated on an individual dwelling basis, which again follows the calculation method in Table 9 of the SAP guidance. This calculation takes account of the heating control type and responsiveness of the system and includes the dwelling HLP in the calculation to account for fabric performance. These set points differ for each dwelling but invariably fall between 18.5 ˚C and 20.5˚ C.

Weather data is also required to calculate annual energy demand. SAP uses single daily average conditions for each month of the year for air temperature, using mean daily values for external air temperature, wind speed, and solar irradiance [48]. Although indicative costs can be calculated using local conditions at a postcode level in SAP, the main calculation for the EPC outputs used weather data for the East Pennine region, which is considered to represent average conditions for the UK [48]. This data was therefore used in all the DEEP model calculations.

In contrast to the steady-state models, DSM calculations use a relatively broad range of inputs at an hourly time-step. These include data for external dry-bulb temperature, relative humidity, direct & diffuse solar irradiance, solar altitude & azimuth, wind speed & direction, and atmospheric pressure. Due to the high resolution of this data, local files are not as readily available as they are for average daily conditions. As simple scheduled infiltration air change rates were used in the DSM models, a monthly control schedule was created to reflect the wind speed-adjusted factors used in the SAP calculations, to allow for fair comparison between annual energy calculations.

The file used in the DSM analysis is for the Leeds city region published by CIBSE. It is approved for use in non-domestic DSM SBEM calculations [49, 50]. A comparison of the relevant mean daily average values for the SAP East Pennine and DSM Leeds weather variables demonstrates a close relationship; with air temperature and wind speed having a similarity of 99.6 % and 99.8 % respectively. For the HTC and annual heating demand calculations, it is primarily the external air temperature that is most relevant. The monthly mean daily external air temperature for the relevant SAP and DSM weather data is illustrated in Figure 4-1. The similarity between the mean daily wind speeds is lower, at 71.4 %. These, however, were only used in SAP as an adjustment to the infiltration heat losses, which were dealt with at an hourly resolution in the DSM models and influenced slightly by external temperature. There was a monthly schedule applied to the total air changes per hour in the DSM models, based on the monthly wind speed factors in the SAP calculations [48]. Wind speed values become more relevant in the DSM models when the more complex air changes through openable windows are considered in the overheating analysis. This is not comparable with SAP due to the dynamic nature of this analysis, however.

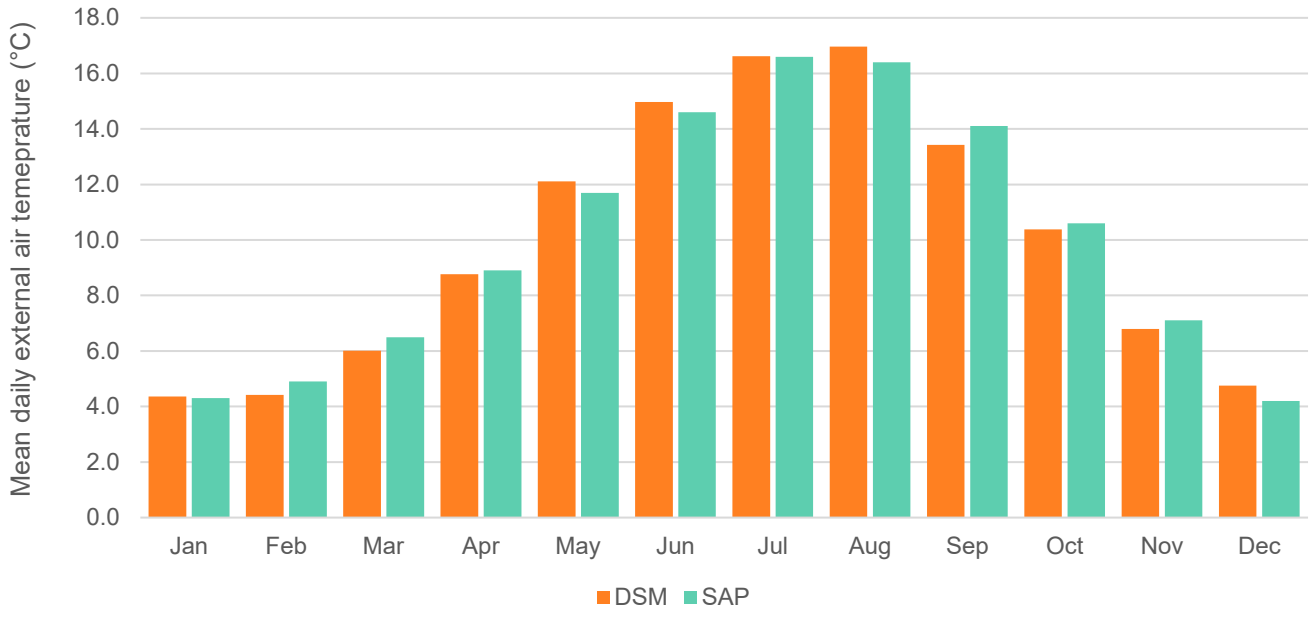

Figure 4-1 Comparison of external air temperature SAP and DSM weather data input

4.3. Comparing measured and modelled HTC accuracy

DEEP investigated the accuracy of building energy modelling by comparing predictions of building heat loss and energy savings resulting from retrofits for each case study with in-situ measurements. To do this the Heat Transfer Coefficient (HTC) is used, which is directly measured during the coheating test [51]. This takes account of heat losses through plane elements, thermal bridges, and infiltration, and provides the most robust metric to understand the whole fabric performance.

The HTC is expressed in watts per kelvin (W/K), which describes the amount of heat required to elevate the internal temperature by 1 K[13]. In steady-state models, the HTC is derived through bottom-up calculations that sum the W/K losses. In contrast, in DSM, models are set-up to mimic the coheating conditions at hourly time-steps, and the HTC is calculated using the same analysis procedure as in the coheating test [44, 52].

The difference between predicted and actual performance is broadly described as the ‘performance gap’ [53-55]. In the field of building performance simulation, how model outputs align with actual performance is commonly referred to as model accuracy and, thus, part of the performance gap can also be attributed to the ‘modelling gap’ [36, 38, 56-59].

Research has shown that retrofit model inputs can be refined to improve the accuracy of post-retrofit energy saving predictions by ‘calibrating’ models with more detailed input data [36, 37, 42-44]. DEEP’s approach to calibration is described in the following section.

4.3.1. Calibrating models to evaluate how default inputs affects EPC accuracy

EPCs for existing buildings are produced using RdSAP, which uses default input data to allow domestic energy assessors to produce EPCs more quickly and simply. This facilitates the production of EPCs where knowledge of the building’s construction is limited. However, there is concern that the use of defaults reduces the accuracy of EPCs, which is especially important when predicting retrofit savings [60].

To investigate this in DEEP, inputs for the energy models are adjusted following a systematic calibration process to refine default data and introduce infiltration rates, U-values, and thermal bridging heat losses (Ψ-values) with specific input data derived from the in-situ tests and thermal modelling. There are many methods of model calibration, and these have been categorised in the past by Reddy [61] as: (a) manual, iterative and pragmatic interventions; (b) informative graphical comparative displays; (c) special tests/analytical procedures; and (d) analytical and mathematical methods. A subsequent review by Coakley at al [36] divides approaches to calibration into two core categories: ‘manual’ and ‘automated’ methods. The method used in the DEEP project can be described as a manual approach, as the fabric inputs are systematically updated using in-situ measured data. It can be further sub-categorized as a ‘procedural extension’ that utilizes an ‘evidence-based development’ method [36].

The method used for DEEP was developed as a simplified means of refining model fabric inputs and calibrating outputs against measured HTC values, having been previously described in peer-reviewed publications [44, 62]. It must be stressed that, although a calibration process is followed to refine inputs, this is based upon the availability of measured air change rates and U-values, and the discrete modelling of linear thermal bridges.

Unlike other more computationally complex methods, this approach does not adjust any remaining inputs to calibrate the final output against the measured HTC; it is used to understand how close the modelled HTC can be to the measured value when more refined data are available. This method was developed using DesignBuilder DSM software, but since RdSAP software has certain restrictions on manipulating model inputs, it is necessary to use BREDEM (the underlying calculation engine behind full SAP and RdSAP), to do this. Part of the motivation for utilising this approach is that it uses modelling tools and a methodology that are used in practice; both SAP and DSM are cited in the PAS 2035 guidance for modelling retrofit performance [63].

Five calibration steps are cumulatively applied in DEEP to each house model at each retrofit stage. From this, the inputs that may be most impactful in achieving accurate predictions can be quantified.

The hierarchy of steps was chosen to reflect the likelihood that real world data may be available as follows and is summarised in Table 4-1. For the infiltration column, the term ‘measured’ is used as shorthand for values approximated from the blower door test results using the n/20 rule of thumb.

The logic for following this hierarchy relates to availability, cost, and time: airtightness tests are readily available and relatively cheap to complete as they are required for new-build regulatory compliance; U-values can be calculated based upon relatively simple site surveys; U-value measurements can be expensive and time consuming to acquire; and a full set of thermal bridging calculations can be time consuming and expensive to produce.

The final two stages could be reversed as both are unlikely to be obtained in practice. However, as there are default y-values and Ψ-values available in SAP, these are considered to be the least likely to be obtained for the purposes of this work.

1. **EPC defaults**: First, the models were run using default values for air infiltration rates, fabric U-values, and thermal bringing heat loss found in RdSAP, which are based on building age bands and construction types [3].This is representative of how most EPCs for existing buildings are determined. Default U-values for building elements are found in Appendix S of RdSAP 2012: version 9.94, with the exception of ground floors, which are calculated according to Section S5.5 of Appendix S of RdSAP 2012 version 9.94. The reason for this is that heat loss via the ground is dependent on the floor construction type and geometry, meaning age band defaults are less useful, and so ground floor U-values are not provided in Appendix S. RdSAP automatically calculates an assumed infiltration rate, based on building characteristics, and it assumes a fixed y-value to account for thermal bridging heat losses based on the building age band.
2. **Measured infiltration**: Next, the models are rerun with the real building infiltration rate input, measured using a blower door test at 50 pascals. From this, air leakage heat loss rates at normal pressures can be approximated using the n/20 rule. In keeping with the RdSAP methodology, a standard sheltered factor of 0.85 is also applied. This was selected as the first calibration step due to the availability and lower cost of the blower door tests. Airtightness testing is also required for all new build homes (under Approved Document Part L of the Building Regulations) and so could be deployed in the market. Currently, infiltration rates cannot be inputted into RdSAP.

3. **Calculated U-values:** In the next step, default U-values for all building elements are swapped with U-values calculated using the BRE U-value calculator, which follows methods defined in BS EN ISO standards [27]. To produce these, measured surveys of the house are needed, possibly involving destructive inspections to explore fabric make-up. Clearly this involves some degree of disruption and costs, as well as expertise to undertake desktop calculations. While the tools allowing U-values to be calculated are available in the retrofit market, currently the practice is not permitted under the RdSAP conventions, and it can be difficult to evidence the element's actual construction build up. However, the facility to override U-values in RdSAP exists if measured U-values are obtained.

4. **Measured U-values**: This step mimics step 3, however, it replaces calculated U-values with U-values derived from in-situ heat flux density measurements undertaken in line with BS ISO 9869-1. Making these measurements requires expertise and has a relatively high cost. There is also substantial room for error in accurately measuring a fabric U-value through spot measurements of a heterogenous fabric element. While possible to make these changes in RdSAP, it is not common practice for a Domestic Energy Assessor to override the default U-values in RdSAP software packages. To do so, assessors would also require suitable qualifications beyond the EPC training course to measure the U-value, and also be able to evidence the element's actual construction build up.

5. **Calculated Ψ-values**: Thermal modelling of bridges is highly specialised, costly, and time consuming. Therefore, it was the last step to be implemented in this process. There are relatively few organisations capable of undertaking the calculations in the UK and they require detailed site surveys and often intrusive inspections in homes. To account for thermal bridging heat loss, RdSAP applies an additional single default y-value to the whole building. It is calculated by multiplying the Ψ-values of thermal bridges by their lengths, adding the products together and dividing by the envelope area. The y-value is measured in W/(m²·K) and may be added to the average U-value to obtain the total rate of heat loss. Default Ψ values for each junction type are used in full SAP and these can be swapped with values generated by thermal modelling software. However, it is not currently possible in RdSAP to input specific Ψ-values for different junctions.

Table 4-1 Modelling calibration steps for each case study building model

Calibration step	Infiltration	U-values	Bridging[2]
1	Default[3]	Default[3]	Default[4]
2	Measured[5]	Default[3]	Default[4]
3	Measured[5]	Calculated[6]	Default[4]
4	Measured[5]	Measured[7]	Default[4]
5	Measured[5]	Measured[7]	Calculated[8]

[2] Bridging calibration can only be applied to BREDEM and DSM
[3] Provided by Appendix S RdSAP 2012 version 9.94
[4] Provided by Appendix K RdSAP 2012 version 9.94
[5] Derived from Blower door test
[6] Derived from BRE Calculator
[7] Derived from Heat flux plate measurements
[8] Calculated from TRISCO bridging simulations

To evaluate the accuracy of the calculated HTC from all models, outputs have been compared with the measured HTC. As noted above, the calibration process includes refined inputs at each stage based upon measurements and discrete modelling of junctions. This does not guarantee that the modelled HTC will be calibrated to match the measured value but does allow for a comparison to be made. It is important to note that compounding errors in some cases can lead to modelled and measured HTCs being similar. However, comparison of measured U-values, and the predicted and measured changes in HTC are used to understand these differences. This is a simplified approach that allows for comparison of the calculated HTC values produced using modelling tools cited in PAS 2035, and readily available in practice [63]. Under coheating conditions and during airtightness testing, all the purpose-provided ventilation paths (extractor fans, chimney, trickle vents etc) are sealed up. The measured HTC, therefore, does not include heat losses from these air exchange mechanisms, i.e. from deliberate ventilation [13]. However, in the SAP calculation, these air exchanges are included in the calculations used to define the HTC, reported in box 39 of the SAP worksheet [3].

To provide a fair comparison of all HTC values, only the air changes related to infiltration have been included in the models used to calculate the HTC. These calculations were all carried out using the BREDEM worksheet with reference to the RdSAP and full SAP guidance [3].

The fabric heat loss (HTC_f), bridging heat loss (HTC_b) and air leakage losses (HTC_v), are outputs of the steady-state software used, though not in DSM. Thus, to disaggregate the heat losses in DSM, the model is run with all inputs active, and then with bridging and infiltration removed respectively, so the individual contribution to the whole house HTCs can be compared.

4.4. EPC improvements, energy, carbon and fuel bill reductions, and payback of retrofits

As with the HTC calculations, models at each stage of calibration described above were used to produce estimates of typical annual energy use pre-retrofit and post-retrofit [11, 44, 64, 65]. Model energy demand outputs were then used to calculate the annual heating cost, carbon dioxide emissions, and EPC rating (following the appropriate SAP and EPC guidance [3, 66]). This was done using all the whole-building modelling tools, to provide a comparison between model outputs. To ensure a fair comparison, all the model inputs related to operation and occupancy were defined following the SAP method.

From this, the annual carbon emissions and annual fuel bill estimates were derived. Along with the retrofit install costs, these were used to estimate simple payback periods for each retrofit, and the success of the retrofits at achieving policy aims evaluated. At this time of uncertain future fuel prices, it is difficult to perform reliable payback calculations, though the underlying energy demand values can be applied to different tariffs at a future date. It is also possible to report the cost reduction as a percentage of the fuel bill to reduce the impact of price rises on the interpretation of the results.

4.5. Overheating analysis using TM59

The detailed overheating analysis carried out by Loughborough University as part of DEEP is supplemented by using the DSM models to evaluate the overheating risk for each case study dwelling, at each stage of retrofit. This was achieved by following the methodology defined in the CIBSE TM59 Design methodology for the assessment of overheating risk in homes [12].

As understanding of domestic overheating has increased, the methods to model and quantify potential overheating have significantly increased in complexity. Initially, a technical memorandum ‘TM52 Limits of Thermal Comfort: Avoiding Overheating in European Buildings’ was published by CIBSE [67] to provide guidance on how overheating can be assessed by practitioners. Subsequently, CIBSE published guidance to simplify the modelling of overheating in dwellings in the document TM59 [12]. It is this methodology that has been used in this work.

In simple terms, the TM59 method introduces a set of operating profiles that simulate the worst-case scenario of continual occupancy under average heatwave conditions. This uses a Design Summer Year (DSY) weather file that is morphed to reflect conditions for the period described as the 2020s. There are, however, three different DSY files available. They use actual year weather data that simulates different heatwave intensities: DSY1 represents a moderately warm summer; DSY2 represents a short, intense warm spell; and DSY3 a longer, less intense, warm spell. These are also morphed to represent expected conditions in the 2020s, 2050s and 2080s as a result of climate change [68].

These files cover low, medium, and high emission scenarios and include probabilistic forecasts within each scenario for the 10th, 50th and 90th percentile [69]. In this work, the DSY1 files for the 2020s, 2050s and 2080s have been used. The 50th percentile in the high emission scenarios (the low emission scenario is now only considered for the 2080s, as current emissions mean that the medium scenario is the lowest viable for the 2050s). In keeping with the energy analysis, the files for the Leeds region have been used.

It is not necessary to repeat the description of the full methodology here as the required model inputs and assumptions are described in detail in the TM59 document. It is, however, useful to note the assessment criteria.

Two criteria are used to assess whether the dwelling may overheat. Criteria A in TM59 is actually adopted from another CIBSE publication, TM52 [67]. The two assessment criteria are defined as follows:

1. For living rooms, kitchens, and bedrooms: the number of hours during which the ΔT (difference between the operative and comfort threshold temperature) is greater than or equal to one degree (K) during the period May to September inclusive shall not be more than 3 % of occupied hours.

2. For bedrooms only: to guarantee comfort during the sleeping hours the operative temperature in the bedroom from 10 pm to 7 am shall not exceed 26 °C for more than 1 % of annual hours. (Note: 1 % of the annual hours between 22:00 and 07:00 for bedrooms is 32 hours).

Whole building models summary

This section describes the steady-state and dynamic models that are being used in DEEP to explore how the retrofits may affect the HTC, energy consumption, carbon emissions, fuel bills, overheating and EPC scores.

A methodology for replacing default data used in RdSAP calculations is proposed, to investigate the implications of using default data in EPCs. This involves up to five stages, using progressively more measured data. Since RdSAP restricts the inputs that can be changed, BREDEM was used to complete the steady-state calibration steps.

The analysis therefore allows comparison between the steady-state and dynamic models, between the different levels of measured input data being used, and against the measured HTC data collected via the in-situ tests.

5. Conclusions

The methodologies proposed for the DEEP case studies have been selected to support a deep dive exploration of the benefits and risks associated with domestic retrofits.

Using multiple research methods to explore the retrofits taking place allows for a richer tapestry of data. This will lead to greater understanding around why certain benefits or risks manifest, what solutions or enhancements may be made to the way that retrofits are modelled and implemented in the UK and provide context to how these may translate across the UK housing stock.

The methodologies proposed have been selected to align with the research plan; so data on other building performance metrics such as: the impact of retrofits on thermal comfort, indoor air quality, humidity and condensation risks, as well as validation of theoretical fuel bill savings was not collected. This would require an alternative research approach involving longitudinal in-use data for occupied homes.

The specific activities undertaken in each of the DEEP case study homes, including the description and discussion of the data collection analysis and interpretations, are published in individual case study reports.

6. References

1. TSB, *Retrofit for the Future, Reducing energy use in existing homes, A guide to making retrofit work*. 2014, Technology Strategy Board: Swindon.
2. HM Government, *Annual Fuel Poverty Statistics in England, 2021 (2019 data)*, E.a.I.S. Department of Business, Editor. 2021, Crown Copyright: London.
3. HM Government, *The Government's Standard Assessment Procedure for Energy Rating of Dwellings, 2012 Edition.*, DECC, Editor. 2014, Building Research Establishment Ltd: Watford.
4. DesignBuilder Software Ltd, *DesignBuilder Version 7.0.0.088*. 2021, DesignBuilder Software Ltd,: Stroud, UK.
5. Haberl, J. and S. Cho, *Literature review of uncertainty of analysis methods*. 2004, Texas Engineering Station, Texas A&M University: Texas.
6. Kelly, S., D. Crawford-Brown, and M.G. Pollitt, *Building performance evaluation and certification in the UK: Is SAP fit for purpose?* Renewable and Sustainable Energy Reviews, 2012. **16**(9): p. 6861-6878.
7. Tupper, K., et al., *Building energy modelling innovation.* Building energy modelling innovation summit, Rocky Mountain Institute, Boulder, 2011.
8. ASHRAE, *Standard 140-2007: Standard method of test for the evaluation of building energy analysis computer programs*. 2007, ASHRAE: Atlanta.
9. CIBSE, *TM33: Tests for Software Accreditation & Verification*. 2006, CIBSE: London.
10. Physibel, *TRISCO. version 14.0w [Software].* 2020, Physibel: Maldegem.
11. HM Government, *PAS 2035:2019 Retrofitting dwellings for improved energy efficiency - Specification and guidance*. 2019, BSI Standards Limited 2019: London.
12. Bonfigli, C., et al., *TM59: Design methodology for the assessment of overheating risk in homes.*, K. Butcher, Editor. 2017, CIBSE: London.
13. Johnston, D., et al., *Whole House Heat Loss Test Method (Coheating).* 2013, Leeds Metropolitan University: Leeds.
14. Sougkakis, V., et al., *Field testing of the QUB method for assessing the thermal performance of dwellings: In situ measurements of the heat transfer coefficient of a circa 1950s detached house in UK.* Energy and Buildings, 2021. **230**.
15. Sougkakis, V., et al., *Evaluation of the precision and accuracy of the QUB/e method for assessing the as-built thermal performance of a low-energy detached house in UK.* Energy and Buildings, 2022. **255**.
16. Alzetto, F., et al., *Comparison of whole house heat loss test methods under controlled conditions in six distinct retrofit scenarios.* Energy and Buildings, 2018. **168**: p. 35-41.
17. HM Government, *Technical Evaluation of SMETER Technologies (TEST) Project*, Department for Business Energy & Industrial Strategy, Editor. 2022, Crown Copyright,: London.
18. ATTMA, *Technical Standard L1A, Measuring Air Permeability of Building Envelopes (Dwellings).* The Air Tightness Testing & Measureemnt Association, Amersham, 2016.
19. CIBSE, *TM23 Testing buildings for air leakage (2022)*. 2022, CIBSE.
20. Roulet, C.-A. and F. Foradini, *Simple and Cheap Air Change Rate Measurement Using CO2 Concentration Decays.* International Journal of Ventilation, 2002. **1**(1): p. 39-44.
21. BSI, *BS ISO 9869-1: Thermal insulation — Building elements — Insitu measurement of thermal resistance and thermal transmittance, Part 1: Heat flow meter method.* British Standards Institute, 2014.
22. Ward, T., *IP 1/06- Assessing the effects of thermal bridging at junctions and around openings*. 2006, The Building Research Establishment: Watford.
23. BSI, *BS EN 13187: Thermal Performance of Buildings - Qualitative Detection of Thermal Irregularities in Building Envelopes - Infrared Method*. 1999, BSI.
24. BRE, *RdSAP 2012 version 9.94 (20th September 2019), Appendix S: Reduced Data SAP for existing dwellings.* BRE, 2019.
25. BRE, *BREDEM A technical description of the BRE Domestic Energy Model Version 1.1*. 2012, BRE: Watford.
26. Ward, T., G. Hannah, and C. Sanders, *Conventions for Calculating Linear Thermal Transmittance and Temperature Factors. BR 497.* 2016, IHS BRE Press: Watford.

27. BRE Ltd, *BRE U-value calculator*. 2007, BRE Ltd: Watford.
28. Deming. W. E., *Statistical Adjustment of Data 1943,*, ed. Wiley. 1985, New York: Dover Publications Edition,.
29. Bacher, P. and H. Madsen, *Identifying suitable models for the heat dynamics of buildings.* Energy and Buildings, 2011. **43**(7): p. 1511-1522.
30. Anderson, B. and L. Kosmina, *Conventions for U-value Calculations. BR 443.* 2019, Building Research Establishment: Watford.
31. BRE, *U-value Calculator. version 2.04g [Software].* 2016, Building Research Establishment: Watford.
32. BSI, *BS EN ISO 10456: 2007 - Building materials and products — Hygrothermal properties - Tabulated design values and procedures for determining declared and design thermal values*, in *British Standards Institute*. 2007.
33. Kornicki., *Air Cavity Calculator. [Software].* n.d., Kornicki: Vienna.
34. Hulme, J., et al., *Solid wall heat losses and the potential for energy saving: The nature of solid walls in situ.* The Building Research Establishment, Watford, 2016.
35. BRE, *The Government's Standard Assessment Procedure for Energy Rating of Dwellings: SAP 2012 Ver: 9.92.* The Building Research Establishment, 2014.
36. Coakley, D., P. Raftery, and M. Keane, *A review of methods to match building energy simulation models to measured data.* Renewable and Sustainable Energy Reviews, 2014. **37**: p. 123-141.
37. Reddy, T., I. Maor, and C. Panjapornpon, *Calibrating detailed building energy simulation programs with measured data – Part I: General methodology.* HVAC&R Research, 2007. **13**(2): p. 221-241.
38. Fabrizio, E. and V. Monetti, *Methodologies and advancements in the calibration of building energy models.* Energies, 2015. **8**(4): p. 2548-2574.
39. Chong, A. and K. Menberg, *Guidelines for the Bayesian calibration of building energy models.* Energy and Buildings, 2018. **174**: p. 527-547.
40. de Wilde, P., *'The building performance gap: Are modellers literate?'.* Building Services Engineering Research and Technology, 2017. **38**(6): p. 757-759.
41. de Wilde, P., *The gap between predicted and measured energy performance of buildings: A framework for investigation.* Automation in Construction, 2014. **41**: p. 40-49.
42. Jankovic, L., *Lessons learnt from design, off-site construction and performance analysis of deep energy retrofit of residential buildings.* Energy and Buildings, 2019. **186**: p. 319-338.
43. Jones, P., et al., *Five energy retrofit houses in South Wales.* Energy and Buildings, 2017. **154**: p. 335-342.
44. Parker, J., et al., *Measuring and modelling retrofit fabric performance in solid wall conjoined dwellings.* Energy and Buildings, 2019. **185**: p. 49-65.
45. Gillich, A., E.M. Saber, and E. Mohareb, *Limits and uncertainty for energy efficiency in the UK housing stock.* Energy Policy, 2019. **133**.
46. HM Government, *UK Building Regulations. Part L1B: Conservation of Fuel and Power in Existing Dwellings* 2014, RIBA Publishing Ltd: London.
47. HM Government, *UK Building Regulations. Part L1A: Conservation of Fuel and Power in New Dwellings* 2014, RIBA Publishing Ltd: London.
48. BRE, *The Government's Standard Assessment Procedure for Energy Rating of Dwellings*. 2014, BRE: Watford.
49. CIBSE, *Leeds Test Reference Year building simulation weather file*. 2016, CIBSE: London.
50. Virk, D. and M. Eames, *CIBSE weather files 2016 release: Technical briefing and testing*. 2016, CIBSE: London.
51. Stafford, A., et al., *Adding value and meaning to coheating tests.* Structural Survey, 2014. **32**(4): p. 331-342.
52. Parker, J.M., D. Farmer, and M. Fletcher. *Calibrating whole house thermal models against a coheating test*. in *System Simulation in Buildings 2014 Proceedings of the Ninth International Conference, December 10-12, 2014.* 2015. Liege: Atelier des Presses.
53. Cuerda, E., et al., *Understanding the performance gap in energy retrofitting: Measured input data for adjusting building simulation models.* Energy and Buildings, 2020. **209**.
54. Johnston, D., D. Miles-Shenton, and D. Farmer, *Quantifying the domestic building fabric 'performance gap'.* Building Services Engineering Research and Technology, 2015. **36**(5): p. 614-627.

55. Zou, P.X.W., et al., *Review of 10 years research on building energy performance gap: Life-cycle and stakeholder perspectives.* Energy and Buildings, 2018. **178**: p. 165-181.
56. Raftery, P., M. Keane, and J. O'Donnell, *Calibrating whole building energy models: An evidence-based methodology.* Energy and Buildings, 2011. **43**(9): p. 2356-2364.
57. Heo, Y., R. Choudhary, and G.A. Augenbroe, *Calibration of building energy models for retrofit analysis under uncertainty.* Energy and Buildings, 2012. **47**: p. 550-560.
58. Badiei, A., D. Allinson, and K.J. Lomas, *Automated dynamic thermal simulation of houses and housing stocks using readily available reduced data.* Energy and Buildings, 2019. **203**.
59. Ji, Y., A. Lee, and W. Swan, *Building dynamic thermal model calibration using the Energy House facility at Salford.* Energy and Buildings, 2019. **191**: p. 224-234.
60. BRE, *Solid wall heat losses and the potential for energy saving; Consequences for consideration to maximise SWI benefits: A route-map for change.* Building Research Establishment, Watford, 2016.
61. Reddy, T., *Literature review on calibration of building energy simulation programs: uses, problems, procedures, uncertainty and tools.* ASHRAE Transactions, 2006(211): p. 226-240.
62. Parker, J., D. Farmer, and M. Fletcher. *Calibrating whole house thermal models against a coheating test*. 2015.
63. BEIS, *PAS 2035:2019: Retrofitting dwellings for improved energy efficiency – Specification and guidance*. 2022, BSI: London.
64. Hall, M.R., et al., *Analysis of UK domestic building retrofit scenarios based on the E.ON Retrofit Research House using energetic hygrothermics simulation – Energy efficiency, indoor air quality, occupant comfort, and mould growth potential.* Building and Environment, 2013. **70**: p. 48-59.
65. Traynor, J., *EnerPHit: A step by step guide to low energy retrofit*. 2019, London: RIBA Publishing.
66. HM Government, *Improving the energy efficiency of our buildings: A guide to Energy Performance Certificates for the construction, sale and let of dwellings.*, D.f.C.a.L. Governance, Editor. 2008, The Staionary Office: Wetherby.
67. CIBSE, *TM52: The limits of thermal comfort: avoiding overheating in European buildings.* . 2013: London.
68. CIBSE. *CIBSE Weather Data Sets*. 2016 11/02/2020]; Available from: https://www.cibse.org/weatherdata.
69. Shamash, M., G. Metcalf, and A. Mylona, *Probabilistic Climate Profiles: The effective use of climate projections in building design*. 2014, CIBSE: London.

This publication is available from: https://www.gov.uk/government/publications/demonstration-of-energy-efficiency-potential-deep

If you need a version of this document in a more accessible format, please email: alt.formats@energysecurity.gov.uk
Please tell us what format you need. It will help us if you say what assistive technology you use.